

MORPHOLOGICAL CONVERGENCE AND
DISPARITY IN THE EVOLUTION OF
TENRECS (AFROSORICIDA, TENRECIDAE)

by

SIVE FINLAY

B.A. (mod), Trinity College Dublin 2012

A thesis submitted in partial fulfillment of
the requirements for the degree of

MASTERS BY RESEARCH

School of Natural Sciences
(Zoology)

Trinity College Dublin

JANUARY 2015

© Sive Finlay, 2015

ABSTRACT

Here is the abstract of my thesis.

TABLE OF CONTENTS

ABSTRACT	ii
TABLE OF CONTENTS	iii
LIST OF TABLES	v
LIST OF FIGURES	vi
ACKNOWLEDGEMENTS	vii
1 INTRODUCTION	1
1.1 Patterns of morphological diversity	1
1.2 Disparity	1
1.3 Convergence	1
1.4 Tenrecs	1
1.5 Structure & contents of this thesis	2
2 METHODS	3
2.1 Introduction	3
2.2 Data collection	4
2.2.1 Species measured and taxonomy	4
2.2.2 Museums' label data	5
2.2.3 Linear measurements	6
2.2.4 Photographing set up	7
2.2.5 Photographing specimens	8
2.2.6 Saving and processing images	10
2.3 Geometric morphometric analyses	10
2.3.1 Landmark placement on images	10
2.3.2 Skulls: dorsal view	12
2.3.3 Skulls: ventral view	13
2.3.4 Skulls: lateral view	14
2.3.5 Mandibles	16
2.3.6 Procrustes superimposition	17
2.4 Error checking	18
2.4.1 Taxonomic	18
2.4.2 Specimen ID	19
2.4.3 Specimen sex and age	19

2.4.4	Linear measurements	20
2.4.5	Potential morphometrics error	21
2.4.6	Landmark placement	22
2.5	Data Analysis	23
2.5.1	Comparing tenrecs' diversity to their closest relatives . . .	23
2.5.2	Quantifying convergence among tenrecs and other small mammals	24
	2.5.2.1 Phylogeny	24
3	RESULTS	26
3.1	Disparity	26
3.1.1	Morphological disparity in tenrecs and golden moles . . .	26
3.1.2	Morphological disparity in non- <i>Microgale</i> tenrecs and golden moles	29
3.2	Convergence	30
4	DISCUSSION	31
4.1	Diversity within tenrecs	31
4.2	Convergence among tenrecs and other small mammals	31
4.3	Future directions	31
4.4	Conclusions	31
	BIBLIOGRAPHY	32

LIST OF TABLES

TABLE 2.1	Summary of species measured	5
TABLE 2.2	Description of the skull and mandible measurements	7
TABLE 2.3	Description of the limb measurements	7
TABLE 2.4	Skulls: dorsal landmarks	13
TABLE 2.5	Skulls: ventral landmarks	14
TABLE 2.6	Skulls: lateral landmarks	16
TABLE 2.7	Mandibles' landmarks	17
TABLE 3.1	Summary of npMANOVA comparisons of morphospace occupation for tenrecs and golden moles	27
TABLE 3.2	Summary of disparity comparisons between tenrecs and golden moles	28
TABLE 3.3	Summary of disparity comparisons between non- <i>Microgale</i> tenrecs and golden moles.	29

LIST OF FIGURES

FIGURE 2.1 Examples of museum labels	6
FIGURE 2.2 Photographic set up	9
FIGURE 2.3 Skulls: dorsal landmarks	12
FIGURE 2.4 Skulls: ventral landmarks	14
FIGURE 2.5 Skulls: lateral landmarks	15
FIGURE 2.6 Mandibles' landmarks	17
FIGURE 3.1 Principal components plots of the morphospaces occupied by tenrecs and golden moles	27

ACKNOWLEDGEMENTS

I would like to acknowledge Dr Rich FitzJohn for letting me use his thesis template!

CHAPTER 1

INTRODUCTION

1.1 PATTERNS OF MORPHOLOGICAL DIVERSITY

Thesis introduction Patterns of diversity, morphological differences, geometric morphometrics overview

1.2 DISPARITY

Exceptional diversity Adaptive radiations and morphological disparity

1.3 CONVERGENCE

Long history of study Repeatability of evolution Methods of measuring convergence

1.4 TENRECS

Phylogenetic history, phenotypic and ecological variety Commonly considered to be both an adaptive radiation and convergent group but this hasn't been tested

CHAPTER 1

1.5 STRUCTURE & CONTENTS OF THIS THESIS

Brief introduction of each section

CHAPTER 2

METHODS

2.1 INTRODUCTION

I compiled a morphological data set of both photographs and linear measurements from 366 specimens representing 101 species of small mammals. I collected morphological data from skulls, limbs and skins and here I included the details of how I compiled each of these data sets. I have only analysed the skulls' data in detail so the information I collected on limbs and skins represent significant resources for future work

I have divided my description of how the data were collected and analysed into four sections:

i Data collection (section 2.2):

Summary of the species measured, information recorded from the museums' labels, linear measurements and photographic set up.

ii Geometric morphometric analyses (section 2.3):

Landmark and semilandmark placements on different views of skulls and mandibles.

iii Error checking (section 2.4):

How I dealt with errors in taxonomic and specimen identification, possible variation associated with sex and age class, accuracy and repeatability of linear measurements and morphometric errors associated with photographing specimens and the placement of landmarks.

iv Quantifying disparity and convergence (section 2.5):

Statistical approaches to measuring patterns of cranial diversity in small mammals.

2.2 DATA COLLECTION

2.2.1 Species measured and taxonomy

Between January and September 2013, I spent a total of 9 weeks working in the collections of five museums: the Natural History Museum London (NHML), the Smithsonian Institute Natural History Museum (SI), the American Museum of Natural History (AMNH), HarvardâŽs Museum of Comparative Zoology (MCZ) and the Field Museum of Natural History (FMNH), Chicago. I compiled measured and photographed 366 skulls, 248 post-cranial skeletons and 277 skins from 101 species belonging to four mammalian orders; Afrosoricida, Erinaceomorpha, Soricomorpha and Notoryctemorphia. These belonged to seven families of mammals; tenrecs (Tenrecidae), golden moles (Chrysochloridae), hedgehogs and gymnures(Erinaceidae), shrews (Soricidae), solenodons (Solenodontidae), moles and desmans(Talpidae) and marsupial moles (Notoryctidae). I measured all of the tenrecs and their sister taxa the golden moles that were available in the collections For my comparative species of non-Afrosoricida species, I chose a random sample of 52 taxa which have been previously identified as convergent with tenrecs (e.g. Gould and Eisenberg, 1966; Symonds, 2005; Poux *et al.*, 2008; Olson, 2013).Following the taxonomy in Wilson and Reeder's Mammal Species of the World (MSW) (2005), I used phylogenies for each order to select species at random which represented the main sub-branches and morphological diveristy of each order. For example, within the Soricomorpha, I included both species of *Solenodon* but only 3 (out of a total of xx) species of

Crocidura as the former genus represents a separate subgroup to the rest of the order.

I used the taxonomy of Wilson and Reeder (2005) supplemented with more recent sources (IUCN, 2012; Olson, 2013) to identify our specimens. Table 2.1 outlines the number of species I measured from each family and how this sample relates to the overall number of species in that group as recorded by both MSW and the IUCN.

TABLE 2.1: The number of species I measured in each family compared to the total number of species in that family according to two sources; (Wilson and Reeder, 2005) and (IUCN, 2012)

Order	Family	Species measured	Species in MSW	Species in IUCN
Afrosoricida	Tenrecidae	X	30	34
Afrosoricida	Chrysochloridae	X	21	21
Erinaceomorpha	Erinaceidae	X	24	X
Soricomorpha	Soricidae	X	376	X
Soricomorpha	Solenodontidae	X	4	X
Soricomorpha	Talpidae	X	39	X
Notoryctemorphia	Notoryctidae	X	2	X

2.2.2 Museums' label data

I recorded all the data on the specimen labels including any handwritten or printed notes which had been added by other users of the collection. The label data included the museum specimen ID number, genus, species, sex, collector's name, the date and location of where the specimen was collected. Some of the labels attached to skins had additional information such as the body, tail, hind foot and ear lengths as well as the body mass of the live individual. The level of detail recorded on the labels varied considerably (figure 2.1). For example recently collected specimens were more likely to have detailed information about the collection location, and some specimens did not have even basic information such as the sex recorded.

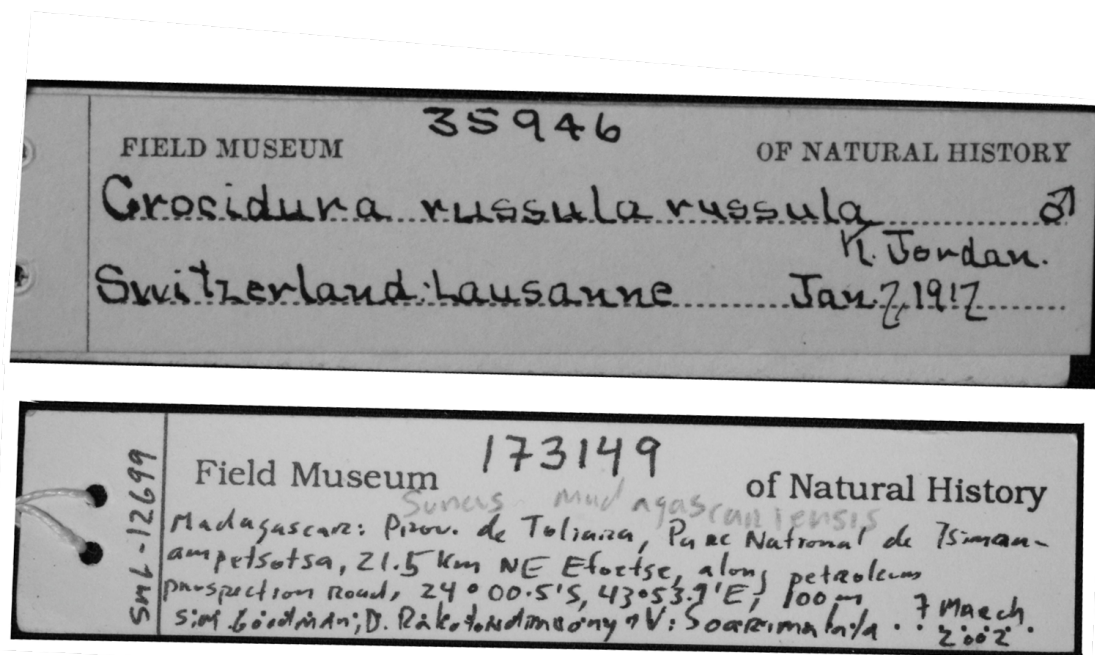


FIGURE 2.1: Examples of the variation in the detail of information which is available from museum labels

2.2.3 Linear measurements

Using a 15mm digital calipers (Mitutoyo Absolute digimatic calipers), I took 20 measurements of the skulls and mandibles (table 2.2) and 19 measurements of the limbs (table 2.3). My choice of which measurements to include was based on three main criteria; 1) their relevance to biological and ecological traits such as diet specialisation and locomotory adaptation, 2) their usefulness for assessing the overall shape and size of the specimen and 3) the ease with which they could be repeated both within and among specimens from different species. Figures x-x depict the linear measurements of skulls and figures xx show the limb measurements.

I took each linear measurement three times, cycling through all 20 skull or 19 limb measurements then repeating the cycle to avoid measuring the same variable twice in a row. Small measurements (<2 mm) are particularly prone

to high error rates (Cardini and Elton, 2008). Therefore, I took five separate replicates of some of the variables which were most prone to errors (marked with PUT IN SYMBOL in tables 2.2 and 2.3). These included four of the skull measurements (PW_a, IncisorH, IFD and IFcanal) and five of the limb measurements (FemD, TibD, HumD, UlnD, RadD). Five replicates should give a more reliable median value because even if there are one or two outlying measurements there should be at least three replicates which are in close agreement (Cooper and Purvis, 2009).

TABLE 2.2: Skull and mandible measurements

Abbreviation	Measurement	Description
---------------------	--------------------	--------------------

TABLE 2.3: Limb measurements

Abbreviation	Measurement	Description
---------------------	--------------------	--------------------

2.2.4 Photographing set up

In order to get 2D landmarks for my specimens, I first had to photograph them. I used photographic copy stands consisting of a camera attachment with an adjustable height bar, a flat stage on which to place the specimen and an adjustable light source to either side of the stage. I used the copy stands that were available at each museum which differed in how the camera height was adjusted and in the light sources available. To take the light variability into account, on each day I took a picture of a white sheet of paper and used the custom white balance function on the camera to set the image as the baseline â€œwhiteâ€ measurement for those particular light conditions.

I photographed the specimens with a Canon EOS 650D camera fitted with either an EF 100mm f/2.8 Macro USM lens (skulls and limbs) or EFS 18-55mm lens (skins). I used a remote control (hähnel Combi TF) to take the photos

to avoid shaking the camera and distorting the images. I photographed the specimens on a black material background. I placed the light source from the top left-hand corner of the picture and positioned a piece of white card on the bottom right side of the specimen which reflected the light back onto the specimen and minimised any shadows (figure 2.2 below).

I made small bean bags (12 x 5cm) from the same black material as the background and filled them with plastic beads. I used these bags as necessary to hold the specimens in position while being photographed. For example, when taking pictures of the lateral view of skulls, I placed one bean bag under the nose of the skull and another bag lying along the top (cranial) side of the skull to ensure that the side I was photographing lay in a flat plane relative to the camera and did not tilt in any direction. I used the grid-line function on the live-view display screen of the camera to position the specimens in the centre of each image.

2.2.5 Photographing specimens

I photographed the skulls in three views; dorsal (top of the cranium), ventral (underside of the skull with the palate roof facing uppermost) and lateral (right side of the skull). I also photographed the outer (buccal) side of the right mandible. When the right side of either the skull or mandibles were damaged or incomplete, I photographed the left sides and later reflected the images so that they could be compared to pictures of the right sides (e.g. Barrow and Macleod, 2008).

Initially, I tried to take pictures of the limbs in similar orientations to the skulls (dorsal, ventral and lateral). However, there was considerable variation in how the limbs were preserved. For example, some limbs were still articulated while others had fragmented bones. It therefore proved impossible to place the limb bones in consistent orientations that would be comparable



FIGURE 2.2: Photographic set up for taking images of my skulls. The camera (above centre) is fitted to a copy stand, the light source is directed from the top-left corner of the image and the white card reflects the light back onto the skull.

across species. Similarly, the small size of some limbs, combined with the frequently incomplete nature of postcranial museum collections, made landmark-based morphometric analyses of any limb pictures impractical. Therefore, I photographed the fore- and hind-limb bones in outer (the side facing away from the rest of the body) and inner (the side facing in towards the centre of the body) views for reference purposes only.

As I was limited by the maximum camera height available on the copy stands, most skins were too large to be photographed with the 100mm macro

lens. Therefore, I used an EFS 18-55mm lens to take pictures of the skins. I photographed skins in the same three orientations as the skulls; dorsal (the upper surface of the animal), ventral (the belly side of the skin) and lateral (right flank of the animal with the skin held in position using bean bags). The dorsal and ventral views give very approximate estimates of the overall body shape of the animal. The lateral views are less biologically relevant since the taxidermic process is unlikely to produce specimens which represent the true body height of the animal.

2.2.6 Saving and processing images

Photographs were captured and saved in a raw file format. Before using the pictures for morphometric analyses, I converted the raw files to binary (grey scale) images and re-saved them as TIFF files. The black and white pictures were more useful for later analyses since I was not interested in including any colour comparisons and it is easier to see some biological features in binary images. TIFF files were the most appropriate to use for my morphometric analyses as they are uncompressed (in comparison to JPEG) images and therefore there is less chance of any picture distortions which may affect later analyses (HERC, 2013).

2.3 GEOMETRIC MORPHOMETRIC ANALYSES

2.3.1 Landmark placement on images

I used a combination of landmark and semilandmark analysis approaches to assess the shape variability in my skull and mandible specimens specimens.

I used the TPS software suite (Rohlf, 2013) to digitise landmarks and curves on my pictures. I set the scale on each pictures individually to standardise for the different camera heights I used when photographing my specimens. I

created separate data files for each of my four morphometric analyses (skulls in dorsal, ventral and lateral views and mandibles in lateral view). I digitised landmarks and semilandmark points on each picture individually.

When combining landmark and semi-landmark approaches, there is a potential problem of over-sampling the curves (REFS). To determine the number of semilandmark points required to adequately summarise the curves in my data sets, I followed the method outlined by MacLeod (2012). For each data set I chose a random selection of pictures of specimens which represented the breadth of the morphological data (i.e. specimens from each sub-group of species). I drew the appropriate curves on each specimen and over-sampled the number of points on the curves. I measured the length of the line and regarded that as the 100%, true length of that outline. I then re-sampled the curves with decreasing numbers of points and measured the length of the outlines. I calculated the length of each re-sampled curve as a percentage of the total length of the curve and then found the average percentage length for that reduced number of semilandamrk points across all of the specimens in my test file. I continued this process until I found the minimum number of points that gave a curve length which was at least 96% accurate. I repeated these curve-sampling tests for each analysis to determine the minimum number of semilandmark points which would give accurate representations of morphological shape.

Here I summarise the landmarks and curves which I used on each of my different sets of pictures. For landmarks which are defined by dental structures, I used published dental formulae (Nowak, 1983; MacPhee, 1987; Knox Jones and Manning, 1992; Marshall and Eisenberg, 1996; Nagorsen, 2002; Goodman *et al.*, 2006; Asher and Lehmann, 2008; ADW, 2013) where available to identify the number and type of teeth in each species.

2.3.2 Skulls: dorsal view

Most of my landmarks in this view are relative (type 3) points which represent overall morphological shape but not necessarily homologous biological features (Zelditch *et al.*, 2012). I placed ten landmarks and drew four semilandmark curves to represent the shape of both the braincase (posterior) and nasal (anterior) area of the skulls (figure 2.3). Table 2.4 describes how I placed the landmarks and drew the outline curves for my dorsal skull pictures

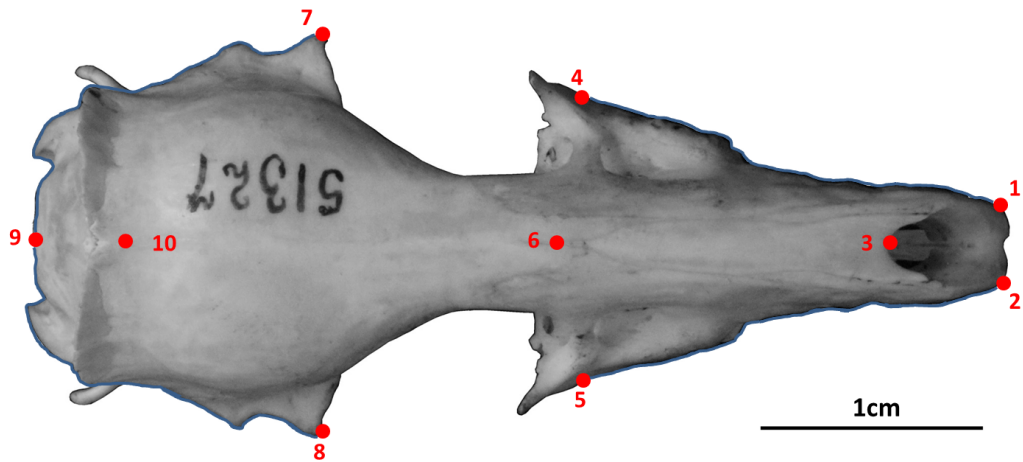


FIGURE 2.3: Landmarks (red) and curves (blue) for the skulls in dorsal view. Curves were re-sampled to the same number of evenly-spaced points. See table 2.4 for description of curves and landmarks. *Potamogale velox* (Tenrecidae) skull, museum accession number: AMNH_51327

TABLE 2.4: Descriptions of the landmarks (points) and curves (semilandmarks) for the skulls in dorsal view (figure 2.3)

Landmark	Description
1 + 2	Left (1) and right (2) anterior points of the premaxilla
3	Anterior of the nasal bones in the midline
4 + 5	Maximum width of the palate (maxillary) on the left (4) and right (5)
6	Midline intersection between nasal and frontal bones
7 + 8	Widest point of the skull on the left (7) and right (8)
9	Posterior of the skull in the midline
10	Posterior intersection between sagittal and parietal sutures
Curve A (12 points)	Outline of the braincase on the left side, between landmarks 9 and 7 (does not include visible features from the lower (ventral) side of the skull)
Curve B (10 points)	Outline of the palate on the left side, between landmarks 4 and 1 (outline of the rostrum only, not the shape of the teeth)
Curve C (12 points)	Outline of the braincase on the right side, between landmarks 9 and 8 (does not include visible features from the lower (ventral) side of the skull)
Curve D (10 points)	Outline of the palate on the right side, between landmarks 5 and 2 (outline of the rostrum only, not the shape of the teeth)

2.3.3 Skulls: ventral view

Most of the landmarks in this view are concentrated around the dentition and palate of the animals. I placed 13 landmarks and drew one outline curve (resampled to 60 semilandmark points) around the back of the skull between landmarks 12 and 13 (figure 2.4). The high variability of my species' basi-cranial region and difficulties associated with identifying developmentally or functionally homologous points precluded designation of additional landmarks towards the back of the skulls. Table 2.5 outlines the descriptions of the landmarks I placed on the ventral pictures.

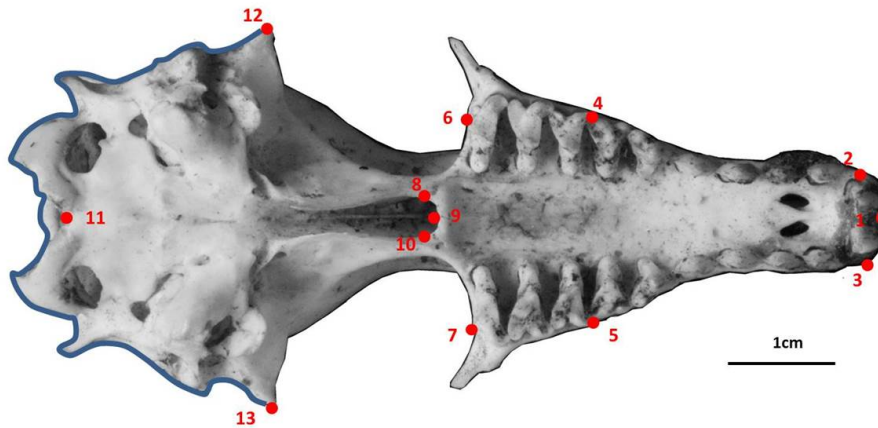


FIGURE 2.4: Landmarks (red) and curve (blue) for the ventral skull pictures, further descriptions in table 2.5. The specimen is a giant otter shrew tenrec, *Potamogale velox*, NHML 1934.6.16.2

TABLE 2.5: Descriptions of the landmarks (points) and curves (semilandmarks) for the skulls in ventral view (figure 2.4)

Landmark	Description
1	Anterior point of the palate
2 + 3	Posterior, lateral extremity of the right (2) and left(3) incisor
4 + 5	Anterior, outer point of the first molar on the right (4) and left (5)
6 + 7	Posterior, outermost point of the molar surface on the right (6) and left (7)
8	Widest point of the curve of the palatine on the right side
9	Posterior point of the palatine in the midline
10	Widest point of the curve of the palatine on the left side
11	Anterior of the occipital foramen in the midline
12 + 13	Widest (extreme lateral) point of the braincase on the right (12) and left (13)
Curve*	Outline of the back of the skull (between landmarks 12 and 13), 60 points

*NB: This curve doesn't necessarily trace homologous features because of the variation in the position of the foramen magnum.

2.3.4 Skulls: lateral view

I placed nine landmarks on the lateral pictures (see figure 2.5 below) and also drew two semilandmark curves between landmarks 7 and 8 to represent the shape of the back of the skull (resampled to 20 semilandmark points) and landmarks 8 and 1 (resampled to 15 semilandmark points) down the midline

of the nose to represent the shape of the top of the skull. Table 2.6 describes my definitions for each of the landmark points. If specimens that were damaged on their right side I reflected photographs of the left lateral side of the skull so that all pictures would be in the same orientation. I originally tried to include more landmarks around the infraorbital foramina (IF) as a crude measure of facial sensitivity and because the IF area is correlated with ecotypes (Crumpton and Thompson, 2012). However, it proved impossible to see the boundaries of the IF in many species and single landmark points could not represent the shape of the full foramina.

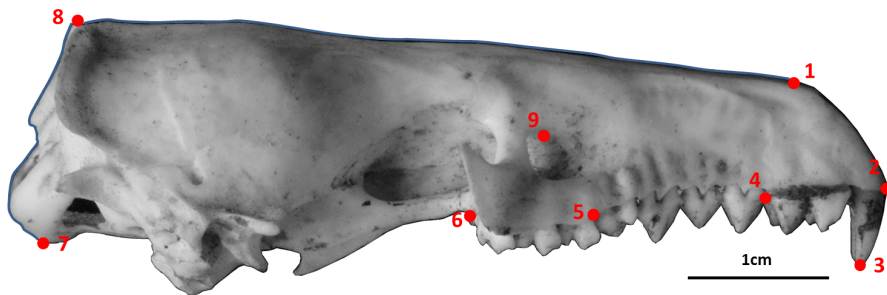


FIGURE 2.5: Landmarks (red) and curve (blue) for the lateral skull pictures, further descriptions in table 2.6. The specimen is a giant otter shrew tenrec, *Potamogale velox*, NHML 1934.6.16.2

TABLE 2.6: Descriptions of the landmarks (points) and curves (semilandmarks) for the skulls in lateral view (see Figure X).

Landmark	Description
1	Anterior, upper tip of the nasal bone
2	Anterior of the alveolus of the first incisor
3	Lowest point of the first incisor
4	Posterior of the alveolus of the last incisor
5	Anterior tip of the alveolus of the first molar
6	Posterior tip of the alveolus of the last molar
7	Lowest point of the basi-occipital (base of the back of the skull)
8	Highest point of the braincase
9	Highest point of the infraorbital foramen
Curve A (20 points)	Between points 7 and 8 Back of the skull from the lowest to highest points
Curve B (15 points)	Between points 8 and 1 From the highest point of the braincase to the front of the nasal

2.3.5 Mandibles

I placed seven landmarks and drew four curves on each mandible picture (again, reflecting any pictures of the left mandible so they could be compared to pictures of the right side). I drew separate curves around each of the three processes of the ascending ramus; coronoid, condyloid and angular and along the base of the horizontal ramus of the jaw. While obviously part of an integrated jaw unit, the development of the mandibular processes are also, in some aspects, independent since they attach different muscles which exert different masticatory forces on the jaw (Barrow and Macleod, 2008). Therefore, by drawing separate curves around each of these elements, my ensuing analyses could assess the relative shape changes of different components of the jaw with relevance to variation in feeding strategies and capabilities.

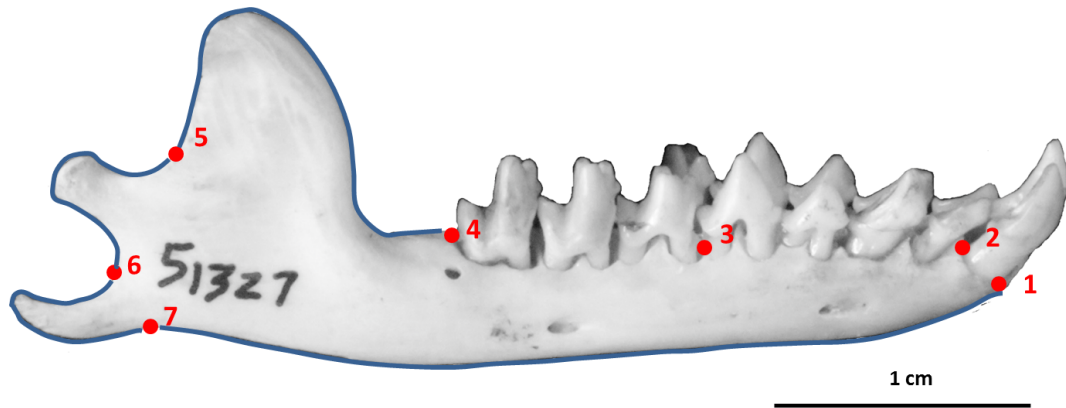


FIGURE 2.6: Landmarks (red) and curves (blue) used for the mandibles. Curves were re-sampled to the same number of evenly-spaced points. See table 2.7 for description of curves and landmarks. *Potamogale velox* (Tenrecidae) mandible, accession number: AMNH_51327

TABLE 2.7: Descriptions of the landmarks (points) and curves (semilandmarks) for the mandibles in lateral (buccal) view (figure 2.6)

Landmark	Description
1	Anterior of the alveolus of the first incisor
2	Posterior of the alveolus of the first incisor
3	Anterior of the alveolus of the first molar
4	Posterior of the alveolus of the last molar
5	Maximum curvature between the coronoid and condylar processes
6	Maximum curvature between the condylar and angular processes
7	Maximum curvature between the angular process and the horizontal ramus
Curve A	Condylloid process (between landmarks 4 and 5, 15 points)
Curve B	Condylar process (between landmarks 5 and 6, 15 points)
Curve C	Angular process (between landmarks 6 and 7, 15 points)
Curve D	Base of the jaw (between landmarks 7 and 1, 12 points)

2.3.6 Procrustes superimposition

After creating my files with the landmarks and semilandmarks placed on each picture, I used TPSUtil (Rohlf, 2012) to create sliders files (Zelditch *et al.*, 2012)

to define which points were semilandmarks. I conducted all further morphometric analyses in R version 3.1.1 (R Core Team, 2014) within the geomorph package (Adams *et al.*, 2013). For each of the separate data sets, we used the gpagen function to run a general Procrustes alignment (Rohlf and Marcus, 1993) of the landmark coordinates while sliding the semilandmarks by minimising procrustes distance (Bookstein, 1997). We used these Procrustes-aligned coordinates of all specimens to calculate average shape values for each species which we then used for a principal components (PC) analysis with the plotTangentSpace function (Adams *et al.*, 2013).

2.4 ERROR CHECKING

My data are prone to a number of different error sources. These include 1) taxonomic identification which has not been updated to currently accepted terms, 2) specimen ID errors, 3) possible variation associated with sex and age class of individuals, 4) the accuracy and repeatability with which species traits are measured, 5) morphometric errors associated with photographing specimens and the placement of landmarks. I address each of these possible sources of error below.

2.4.1 Taxonomic

I recorded species names as they were written on museum specimen labels and then corrected them to match the taxonomy in Wilson and ReaderâŽs Mammal Species of the World (2005). For recently identified species, such as *Microgale jobihely* (Goodman *et al.*, 2006), which are not included in Wilson and Reader (2005), I used the taxonomy recorded on the labels.

2.4.2 Specimen ID

There were four specimens from the Smithsonian Institute that had species labels which did not match between skulls and skins with the same specimen ID numbers. The four skulls were labelled as *Hemicentetes semispinosus*. The corresponding skins were originally labelled as *H. semispinosus* but this was crossed out and changed to *H. nigriceps*. The re-labelled skins looked clearly different to the undisputed *H. semispinosus* skins and also look more similar to other pictures of *H. nigriceps*. Therefore, I made the assumption that the re-labelling of the skins as *H. nigriceps* represents the true taxonomy and I treated the corresponding skulls as *H. nigriceps*.

2.4.3 Specimen sex and age

Information about the sex and/or age of an individual is often missing from museum records. Mammalian species can often be identified as juveniles by looking for incomplete fusion of the crania and non-fully erupted dentition (REFS) However, age classification in tenrecs is difficult using these criteria; in some species, the last molar does not erupt fully until the first molar has been shed so the full dentition is never present at any one time (Nowak, 1983). It is also difficult to distinguish deciduous from permanent teeth in *Microgale* tenrecs (Asher and Lehmann, 2008) which has led to confusion and misidentification of juvenile forms as separate species (Olson *et al.*, 2004). I excluded any obvious juvenile specimens from my data set. Where specimens could not be obviously identified as juveniles I treated them all as equivalent adult forms. I included both male and female specimens in my data as significant sexual dimorphism in skull or body size has not been identified in any of my species (REFS Olson *et al.*, 2004).

2.4.4 Linear measurements

As mentioned above (section 2.2.3), I took three replicate measurements of most of my variables and five replicates of other variables. Some morphometric studies take replicate measurements of a trait and use the average value for further analyses (REFS). Rather than taking the mean of each of three (or five) measures, I used the median as it is less likely to be skewed by outliers and gives a more accurate representation of the true value of the trait (REFS?). Before extracting the median values I followed the protocol for assessing measurement error outlined by (Cooper and Purvis, 2009). This method assesses whether there is a reasonable correlation among the replicate measurements of the same variable. The error checking criteria are based on two calculations; the coefficient of variation and the percentage spread.

I calculated the coefficient of variation (standard deviation/mean*100) for each measurement. This value estimates the extent to which replicate measurements deviate from the mean. When the coefficient of variation was less than 5%, I accepted the median value as an accurate measurement of the size of the structure. If the coefficient of variation was greater than 5%, indicative of a low agreement between replicate measurements, I measured the percentage spread of the data. For variables measured three times, I calculated percentage spread as $[(\text{minimum difference between neighbouring measurements}) / (\text{range of measured values}) * 100]$. For variables that I measured five times, the differences between neighbouring values were calculated and labelled from smallest to largest as a, b, c, and d with the range of the measured values designated as e (Cooper and Purvis, 2009). For these variables, I calculated percentage spread as $[(a/e + b/e + c/e) * 100]$. Small percentage spread values indicate close agreement between repeated measurements. When percentage spread approaches 50% the data are evenly spread out and therefore there is no way of knowing whether the median value is an accurate measurement of the

trait (Cooper and Purvis, 2009). I chose to use 25% as a cut off point for accepting the accuracy of measured traits.

I used these error checking criteria to assess the accuracy of my repeated measurements of both skulls and limbs.

2.4.5 Potential morphometrics error

I used 2D morphometrics to compare the morphologies of the skulls (section 2.3). The small size of my specimens, combined with the number of specimens involved in my study made 3D imaging impractical. It takes roughly 1.5 hours for a good quality scan of each specimen so it would have taken me at least 550 hours to scan the 366 specimens that I photographed.

While 2D methods are an accepted means of comparing morphological shape (e.g. Adams *et al.*, 2004; Mitteroecker and Gunz, 2009), particularly for comparing skull morphologies of small mammals (e.g. Cardini, 2003; Panchetti *et al.*, 2008; White and Searle, 2008; Barrow and Macleod, 2008; Scalici and Panchetti, 2011), the inherent discrepancies associated with comparing three dimensional objects using two dimensional pictures do introduce some difficulties of possible distortion of the image (Arnqvist and Mårtensson, 1998). Similarly, human error with how landmarks are positioned on specimens could also introduce noise into further analyses. In contrast to detailed intraspecific work (REFS) photographic or landmark placement errors are unlikely to be significant in interspecific studies since one would expect that the morphological variation among species is large enough to be detected as a signal above any background noise associated with methodological error (REFS). Nevertheless, it is still important to assess measurement error in a morphometric data set to increase confidence in the outcome of final analyses. I identify two main sources of morphometric measurement error; specimen orientation and placement of landmarks.

Variation in the orientation of specimens for photography is one of the main sources of error in 2D morphometric studies (Adriaens, 2007). If specimens are not placed on a flat plane or in a consistent position relative to the camera, areas of the object which are tilted towards the camera will appear to be larger than reality, distorting any subsequent morphometric analyses of the shape. I used a random subset of skulls comprised of one representative from each of my 89 species to estimate the overall specimen orientation error in my photographic dataset. This subset included representatives from each tenrec and golden mole species along with samples from my comparative species (total of xx moles, xx shrews, xx hedgehogs ...) I took three sets of pictures of each view of the skulls and mandibles, cycling through the pictures so that the specimen was removed and re-positioned before every shot (Viscosi and Cortini, 2011).

2.4.6 Landmark placement

I placed the landmarks on each set of pictures so inter-observer variation is not an issue for my study. However, repeatability and reliability of my choice of landmarks could affect the final results of my analyses (Arnqvist and Mårtensson, 1998). I used a combined, nested approach to test for both orientation and landmark placement error (Arnqvist and Mårtensson, 1998; Barrow and Macleod, 2008). For each of the 89 specimens in my random subset of species, I photographed their skulls (dorsal, ventral and lateral views) and mandibles three times. I then copied these images and placed landmarks on 3 copies of each image. I used a nested mixed mode ANOVA to assess the measurement error of the Procrustes-superimposed coordinates. There were three factors in my ANOVA; specimen, photo (3 pictures of each specimen) and landmark trial (placed landmarks on 3 copies of each of my photos).

2.5 DATA ANALYSIS

Introduction to the data analyses

2.5.1 Comparing tenrecs' diversity to their closest relatives

For each of the morphometric data sets (dorsal, ventral, lateral skulls and mandibles), I ran a general Procrustes alignment (section 2.3.6) of just my tenrec and golden mole specimens to compare morphological diversity in the two families. I used the principal components axes which accounted for 95 % of the cumulative variation to calculate four disparity metrics; the sum and product of the range and variance of morphospace occupied by each family (Brusatte *et al.*, 2008; Foth *et al.*, 2012; Ruta *et al.*, 2013). We also calculated morphological disparity directly from the Procrustes-superimposed shape data based on the sum of the squared inter-landmark distances among species pairs (SSqDist, Zelditch *et al.*, 2012).

I used two approaches to test whether tenrecs have significantly different morphologies compared to golden moles. The first was a comparison of morphospace occupation between the two groups with non parametric MANOVAs (Anderson, 2001) to test whether tenrecs and golden moles occupy significantly different areas of morphospace (e.g Serb *et al.*, 2011; Ruta *et al.*, 2013).

Secondly, I used pairwise permutation tests to test the null hypothesis that tenrecs and golden moles have equal disparity. If this hypothesis were true then the designation of each species as belonging to either tenrecs or golden moles should be arbitrary because each group would have the same disparity. Therefore I permuted the data by assigning family identities at random to each specimen and calculated the differences in disparity for each of the new family groupings. I repeated these permutations 1000 times to generate a null distribution of the expected differences in family disparity. I compared the observed (true) measures of the differences in disparity between tenrecs and

golden moles to these permuted distributions to test whether the families had significantly different levels of disparity.

The majority of tenrec species (19 out of 31 in my data) are members of the *Microgale* (shrew-like) genus which is notable for its relatively low phenotypic diversity (Soarimalala and Goodman, 2011; Jenkins, 2003). The strong similarities among these species may mask signals of higher disparity among other tenrecs. Therefore I repeated my family-level comparisons of disparity with a reduced data set that excluded the *Microgale* so that I could compare disparity within the remaining 12 tenrec species to disparity within the 12 species of golden moles.

2.5.2 Quantifying convergence among tenrecs and other small mammals

PHYLOGENY — Instead of basing my analyses on individual trees and assuming that their topologies are known without error (e.g. Ruta *et al.*, 2013; Foth *et al.*, 2012; Brusatte *et al.*, 2008; Harmon *et al.*, 2003) I used a distribution of 101 pruned phylogenies derived from the randomly resolved mammalian supertrees in (Kuhn *et al.*, 2011).

Eight species (six *Microgale* tenrecs and two golden moles) in my morphological data sets were not in the phylogenies. Phylogenetic relationships among the *Microgale* have not been resolved more recently than the (Kuhn *et al.*, 2011) analysis, therefore I added the additional *Microgale* species at random to the *Microgale* genus within each phylogeny (Revell, 2012). I could not use the same approach to add the two missing golden mole species because they were the only representatives of their respective genera within my data. Therefore I randomly added these species to the common ancestral node (using the find-MRCA function in phytools (Revell, 2012)) of all golden moles within each phylogeny. Adding these extra species to the phylogenies created polytomies which I resolved arbitrarily using zero-length branches (Paradis *et al.*, 2004). I

calculated pairwise phylogenetic distances among species using the cophenetic function (R Core Team, 2014).

CHAPTER 3

RESULTS

Overall results summary

3.1 DISPARITY

When we compared tenrecs' cranial morphologies to their closest relatives we found a trend towards higher disparity in tenrecs than in golden moles. However, these apparent differences were only significant for some disparity metrics. In contrast, golden moles have more diverse mandible shapes than tenrecs which appears to be due to greater morphological variety in the posterior mandible structures of golden moles (section 3.1.2).

3.1.1 Morphological disparity in tenrecs and golden moles

Figures 3.1 depict the morphospace plots derived from our principal components analyses of average Procrustes-superimposed shape coordinates for each species in our skull and mandible data respectively. We used the principal components axes which accounted for 95% of the cumulative variation ($n = 7, 8, 8$ axes for the dorsal, ventral and lateral skull analyses respectively and $n = 12$ axes for the mandibles) to calculate the disparity of each family.

Tenrecs and golden moles clearly have very different cranial and mandible morphologies: in each analysis, the families occupy significantly different areas of morphospace (npMANOVA, table 3.1).

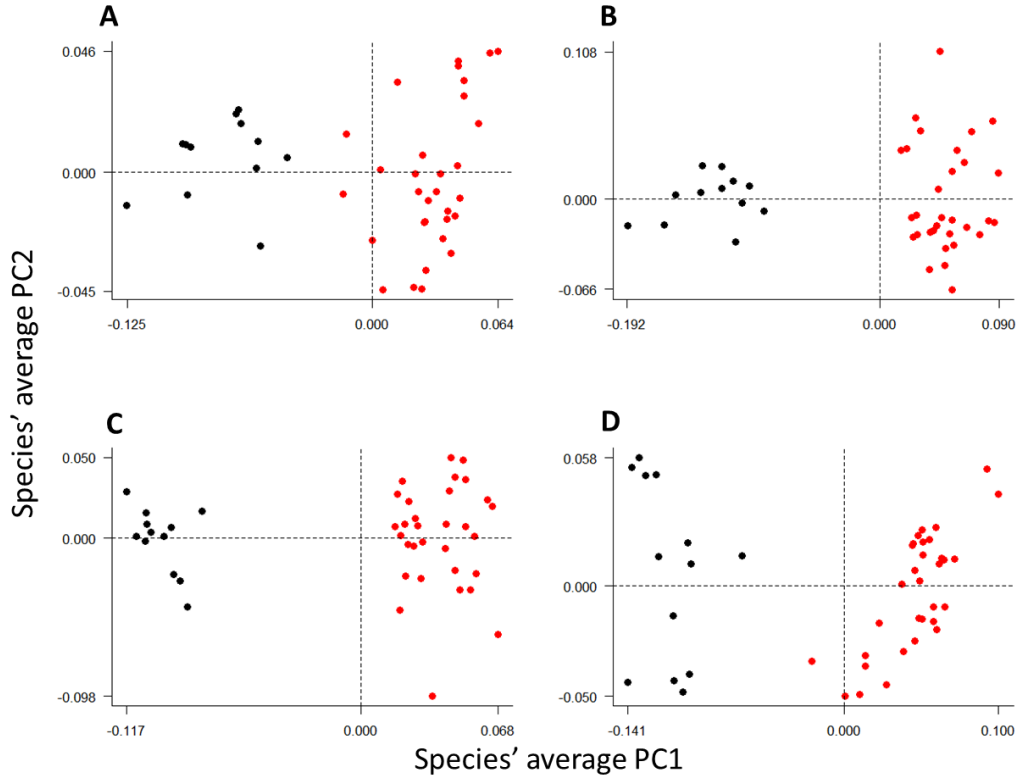


FIGURE 3.1: Principal components plots of the morphospaces occupied by tenrecs (red, $n=31$ species) and golden moles (black, $n=12$) for the skulls: dorsal (A), ventral (B), lateral (C) and mandibles (D) analyses. Axes are PC1 and PC2 of the average scores from a PCA analysis of mean Procrustes shape coordinates for each species.

TABLE 3.1: Summary of the npMANOVA comparisons of morphospace occupation for tenrecs and golden moles in each of the four analyses (three views of skulls and mandibles). In each case the two families occupy significantly different areas of morphospace.

Analysis	F	R ²	p value
Skulls dorsal	66.02	0.62	0.001
Skulls ventral	100.74	0.71	0.001
Skulls lateral	75.07	0.65	0.001
Mandibles	59.34	0.59	0.001

Our comparisons of disparity levels within each family yielded different trends for the skulls compared to the mandible analyses. In our analyses of the three different views of the skulls, when disparity is calculated from principal component - based metrics there is an overall trend for tenrecs to have higher disparity than golden moles. However, none of these differences are statistically significant (table 3.2). In contrast, when we calculated disparity based on the sum of squared interlandmark differences between species pairs (Zelditch *et al.*, 2012) then golden moles had significantly higher levels of disparity than tenrecs (table 3.2).

TABLE 3.2: Summary of disparity comparisons between tenrecs (T) and golden moles (G) for each of the data sets(rows) and five disparity metrics (columns). "Mandibles:one curve" refers to my shape analysis of mandibles excluding the three curves around the posterior structures of jaw (figure 2.5). Significant differences are highlighted in bold with the corresponding p value in brackets. Disparity metrics are; sum of variance, product of variance, sum of ranges, product of ranges and sum of squared distances among species.

Disparity metric	SumVar	ProdVar	SumRange	ProdRange	SSqDist
Skulls dorsal	T>G	T>G	T>G	T>G	G>T* (0)
Skulls lateral	T>G	T>G	T>G	T>G	G>T* (0)
Skulls ventral	T>G	G>T	T>G	T>G	G>T* (0)
Mandibles	G>T	G>T* (0.008)	T>G* (0.025)	T>G* (0.009)	T>G* (0)
Mandibles	G>T	G>T	T>G	T>G	T>G* (0)

There is a less clear pattern from our analysis of disparity in the mandibles. Three of our five metrics indicate that golden moles have significantly higher disparity in the shape of their mandibles than tenrecs (table 3.2) although one metric (sum of ranges) indicated the opposite result.

The three curves that we placed at the back of the mandibles (figure 2.6) place a particular emphasis on shape variation in the posterior of the bone; the ramus, coronoid, condylar and angular processes. Therefore, higher disparity in golden mole mandibles compared to tenrecs could be driven by greater

morphological variation in these structures. To test this idea, we repeated our morphometric analyses of the mandibles with a reduced data set of points; just the seven landmark points and one single curve at the base of the jaw between landmarks 1 and 7 (figure 2.6). When we compared familial disparity levels with this reduced data set we found that golden moles no longer had significantly higher disparity than tenrecs but rather there were some indications that the opposite was true (table 3.2).

3.1.2 Morphological disparity in non-*Microgale* tenrecs and golden moles

We repeated our disparity comparisons with a subset of the tenrec specimens to remove the large and phenotypically similar *Microgale* tenrec genus. In this case we found that tenrecs have significantly higher disparity than golden moles when the skulls are analysed in lateral view (table 3.3). However, none of the other comparisons in any of the analyses were significant. Similarly, the trend in the main analysis for golden moles to have significantly higher disparity measured as the sum of squared inter-landmark distances (table 3.2) was not repeated in this comparison of disparity in non-*Microgale* tenrecs and golden moles (table 3.3).

TABLE 3.3: Summary of disparity comparisons between non-*Microgale* tenrecs (T) and golden moles (G) for each of the data sets(rows) and five disparity metrics (columns). Significant differences are highlighted in bold with the corresponding p value in brackets. Disparity metrics are; sum of variance, product of variance, sum of ranges, product of ranges and sum of squared distances among species.

Disparity metric	SumVar	ProdVar	SumRange	ProdRange	SSqDist
Skulls dorsal	T>G	T>G	T>G	T>G	T>G
Skulls lateral	T>G* (0.014)	T>G	T>G* (0.001)	T>G*(0.003)	G>T* (0.014)
Skulls ventral	T>G	T>G	T>G	T>G	T>G
Mandibles	T>G	G>T	T>G	G>T	G>T

CHAPTER 3

3.2 CONVERGENCE

CHAPTER 4

DISCUSSION

Overall summary of points and implications of findings

4.1 DIVERSITY WITHIN TENRECS

They don't seem to be more diverse than their closest relatives

4.2 CONVERGENCE AMONG TENRECS AND OTHER SMALL MAMMALS

4.3 FUTURE DIRECTIONS

Simulations, ecological convergence, measure adaptiveness, more detailed echolocation studies?

4.4 CONCLUSIONS

BIBLIOGRAPHY

- Adams D., Otárola-Castillo E., and Paradis E. 2013. geomorph: an r package for the collection and analysis of geometric morphometric shape data. *Methods in Ecology and Evolution* 4:393–399.
- Adams D.C., Rohlf F.J., and Slice D. 2004. Geometric morphometrics: Ten years of progress following the "revolution". *Italian Journal of Zoology* 71:5–16.
- Adriaens D. 2007. Protocol for error testing in landmark based geometric morphometrics.
- ADW. 2013. Animal diversity web.
- Anderson M. 2001. A new method for non-parametric multivariate analysis of variance. *Austral Ecology* 26:32–46.
- Arnqvist G. and Mårtensson T. 1998. Measurement error in geometric morphometrics; empirical strategies to assess and reduce its impact on measures of shape. *Acta Zoologica Academiae Scientiarum Hungaricae* 44:73–96.
- Asher R.J. and Lehmann T. 2008. Dental eruption in Afrotherian mammals. *BMC Biology* 6.
- Barrow E. and Macleod N. 2008. Shape variation in the mole dentary (Talpidae: Mammalia). *Zoological Journal of the Linnean Society* 153:187–211.
- Bookstein F. 1997. Landmark methods for forms without landmarks: morphometrics of group differences in outline shape. *Medical image analysis* 1:225–243.
- Brusatte S., Benton M., Ruta M., and Lloyd G. 2008. Superiority, competition and opportunism in the evolutionary radiation of dinosaurs. *Science* 321:1485–1488.
- Cardini A. 2003. The geometry of the marmot (Rodentia: Sciuridae) mandible: phylogeny and patterns of morphological evolution. *Systematic Biology* 52:186–205.
- Cardini A. and Elton S. 2008. Does the skull carry a phylogenetic signal? Evolution and modularity in the guenons. *Biological Journal of the Linnean Society* 93:813–834.

- Cooper N. and Purvis A. 2009. What factors shape rates of phenotypic evolution? A comparative study of cranial morphology of four mammalian clades. *Journal of Evolutionary Biology* 22:1024–1035.
- Crumpton N. and Thompson R. 2012. The holes of moles: Osteological correlates of the trigeminal nerve in *Talpidae*. *Journal of Mammalian Evolution*.
- Foth C., Brusatte S., and Butler R. 2012. Do different disparity proxies converge on a common signal? Insights from the cranial morphometrics and evolutionary history of *Pterosauria* (Diapsida: Archosauria). *Journal of Evolutionary Biology* 25:904–915.
- Goodman S.M., Raxworthy C.J., Maminirina C.P., and Olson L.E. 2006. A new species of shrew tenrec (*Microgale jobihely*) from northern Madagascar. *Journal of Zoology* 270:384–398.
- Gould E. and Eisenberg J.F. 1966. Notes on the biology of the Tenrecidae. *Journal of Mammalogy* 47:660–686.
- Harmon L., Schulte J., Larson A., and Losos J.B. 2003. Tempo and mode of evolutionary radiation in iguanian lizards. *Science* 301:961–964.
- HERC U.B. 2013. RHOI Fossil Photography Protocol.
- IUCN. 2012. International Union for Conservation of Nature.
- Jenkins P. 2003. *Microgale*, shrew tenrecs, pages 1273–1278. The University of Chicago Press, Chicago.
- Knox Jones J. and Manning R. 1992. Insectivores.
- Kuhn T., Mooers A., and Thomas G. 2011. A simple polytomy resolver for dated phylogenies. *Methods in Ecology and Evolution* 2:427–436.
- MacLeod N. 2012. Going Round the Bend ii: Extended Eigenshape Analysis.
- MacPhee R. 1987. The shrew tenrecs of Madagascar: Systematic revision and holocene distribution of *Microgale* (Tenrecidae, Insectivora). American Museum Novitates Number 2889:1–45.
- Marshall C. and Eisenberg J.F. 1996. *Hemicentetes semispinosus*.
- Mitteroecker P. and Gunz P. 2009. Advances in geometric morphometrics. *Evolutionary Biology* 36:235–247.
- Nagorsen D. 2002. An identification manual to the small mammals of British Columbia.
- Nowak R. 1983. *Walker's Mammals of the World*, 4th edition, vol. 1. Johns Hopkins University Press, Baltimore.

BIBLIOGRAPHY

- Olson L., Goodman S., and Yoder A. 2004. Illumination of cryptic species boundaries in long-tailed shrew tenrecs (Mammalia: Tenrecidae; *Microgale*), with new insights into geographic variation and distributional constraints. *Biological Journal of the Linnean Society* 83.
- Olson L.E. 2013. Tenrecs. *Current Biology* 23:R5–R8.
- Panchetti F., Scalici M., Carpaneto G., and Gibertini G. 2008. Shape and size variations in the cranium of elephant-shrews: a morphometric contribution to a phylogenetic debate. *Zoomorphology* 127:69–82.
- Paradis E., Claude J., and Strimmer K. 2004. Ape: Analyses of Phylogenetics and Evolution in R language. *Bioinformatics* 20:289–290.
- Poux C., Madsen O., Glos J., de Jong W.W., and Vences M. 2008. Molecular phylogeny and divergence times of Malagasy tenrecs: Influence of data partitioning and taxon sampling on dating analyses. *BMC Evolutionary Biology* 8.
- R Core Team. 2014. R: A Language and Environment for Statistical Computing. R Foundation for Statistical Computing, Vienna, Austria.
- Revell L. 2012. phytools: an R package for phylogenetic comparative biology (and other things). *Methods in Ecology and Evolution* 3:217–223.
- Rohlf F. 2012. Tpsutil.
- Rohlf F. 2013. Tpsdig2 ver 2.17.
- Rohlf J. and Marcus L. 1993. A revolution in morphometrics. *Trends in Ecology & Evolution* 8:129–132.
- Ruta M., Angielczyk K., Fröbisch J., and Benton M. 2013. Decoupling of morphological disparity and taxic diversity during the adaptive radiation of anomodont therapsids. *Proceedings of the Royal Society B: Biological Sciences* 280:20131071.
- Scalici M. and Panchetti F. 2011. Morphological cranial diversity contributes to phylogeny in soft-furred sengis (Afrotheria, Macroscelidea). *Zoology* 114:85–94.
- Serb J., Alejandrino A., Otárola-Castillo E., and Adams D. 2011. Morphological convergence of shell shape in distantly related scallop species (mollusca: Pectinidae). *Zoological Journal of the Linnean Society* 163:571–584.
- Soarimalala V. and Goodman S. 2011. Les petits mammifères de Madagascar. Guides sur la diversité biologique de Madagascar, Association Vahatra, Antananarivo, Madagascar.
- Symonds M.R.E. 2005. Phylogeny and life histories of the "Insectivora": controversies and consequences. *Biological Reviews* 80:93–128.

BIBLIOGRAPHY

- Viscosi V. and Cortini A. 2011. Leaf morphology, taxonomy and geometric morphometrics: a simplified protocol for beginners. PLOS One 6:e25630.
- White T. and Searle J. 2008. Mandible asymmetry and genetic diversity in island populations of the common shrew, *Sorex araneus*. Journal of Evolutionary Biology 21:636–641.
- Wilson D. and Reeder D. 2005. Mammal species of the world. A taxonomic and geographic reference (3rd ed). Johns Hopkins University Press.
- Zelditch M., Swiderski D., and Sheets D. 2012. Geometric Morphometrics for Biologists, second edition. Academic Press, Elsevier, United States of America.